Dynamics of a High Molecular Weight PS−PMMA Diblock Copolymer in Mixed Selective Solvents. 1. Unimer−Micelle Coexistence

Yoshisuke Tsunashima* and Sinji Suzuki†

Institute for Chemical Research, Kyoto University, Uji, Kyoto 611-0011, Japan

Received: April 22, 1999

Dynamic and static light scattering and viscosity measurements were made for a polystyrene (PS)−*block*-poly(methyl methacrylate) (PMMA) of high molecular weight $M_w = 1.53 \times 10^6$ (38.5 wt % PS) in mixed selective solvents of benzene/*p*-cymene at 30.0 °C, where benzene was good to PS and PMMA, while *p*-cymene was good to PS but poor/precipitant to PMMA. In a solvent of benzene/*p*-cymene = 40/60 (v/v), the block copolymer formed a monodispersed micelle and the micelle coexisted with the single copolymer (unimer) in the quiescent state. The micellization due to the weak segregation led the micelle to a thermodynamically equilibrium size of *loose* association, which is composed of three pieces of unimers. However, the micelle broke into unimers under the shear rate of 1700−2000 s^{-1} in the capillary viscometer. This feature was caused by the flabby structure of the micelle characterized dynamically by the vast motions occurring inside the micelle. With strong preferential adsorption of *p*-cymene to the PS shell part and with a limited amount of benzene in the PMMA core part, the intramicellar motions became much more active than the case of usual flexible linear polymers in good solvents. The micelle structure was thus well represented by the soft-core/Gaussian chain shell model, not by the hard-core shell model.

Introduction

So far the chain dynamics of diblock copolymers in dilute solution has not been studied much theoretically[1−6] or experimentally.[7−11] Here the chain dynamics means the diffusion motion and the internal modes of motion. Both motions in diblock copolymers are affected by the hydrodynamic interaction operating not only on the individual subchain but also on the pairs of different subchains, the latter interaction being particular to the diblock chains. In good solvents for both subchains, the block copolymer was found to suffer the strong intrachain hydrodynamic interaction because of the vast hydrodynamic heterocontacts between different subchain elements.[9,10] As a result, the center-of-mass diffusion of an entire copolymer molecule is retarded by the hydrodynamic coupling of the internal motions with the diffusion motion, and the nondraining hydrodynamic nature represented by q^3 dependence of the first cumulant is attained in a remarkably small qR_G region as $qR_G = 1$. Here R_G is the root-mean-square radius of gyration of the chain. In selective organic solvents, however, the chain dynamics has little been investigated from the viewpoint of chain dynamics mentioned above. The reasons are that the diblock copolymers studied are of molecular weight as small as $5\sim10 \times 10^4$ or 2×10^5 at most, and they form spherical intermolecular micelles with large association numbers.[12−18] These diblock copolymers show an amphiphilic nature and behave as a low molecular weight surfactant in dilute solution, that is, the micelles are in a nearly monodispersed state in mass and size, and are composed of a poorly soluble compact core and of a soluble surrounding corona. The micellar structures can be explained without any hindrance by spherical particles of rigid and concentric density distribution. Thus, internal motions are completely out of the question, and the micelle sizes and/or the micellization are the points to be discussed, instead.[12−18]

Following, it will be expected that as the molecular weight of diblock copolymers increases, the micelles formed in selective solvents show behavior quite different in both dynamics and structure from that for usual micelles of medium molecular weights mentioned above. The increase in the soluble subchain length will induce the increase in the internal mobility of micelles or reduce the structural rigidity of micelles, whereas the increase in the insoluble subchain length will make the core stiffness sensitive to the quality of selective solvents. Both changes are effective to make the intramicellar motions vigorous and detectable. These internal motions in selective solvents, however, are expected to be quite different from those in good solvents, because the internal motions of the insoluble subchain are constrained in the core to some extent, depending on the solvent quality. Thus, the hydrodynamic heterocontacts, or the composition fluctuation between different subchain elements inside the micelle, which are predominant in good solvents,[9,10] will be depressed and rather the heterocontacts between the insoluble core and the soluble subchain elements will become more effective. The latter might induce a very slow motion or an agitating motion of the core in the soluble subchain space. Such very slow concentration fluctuations in the micelle might modulate or accelerate the internal motions of the soluble subchain. These modes of motions are detectable only for micelles that are composed of high molecular weight diblock copolymers.

In this paper (series 1) and a forthcoming one (series 2),[19] we aimed to investigate the dynamic motions and structures of a high molecular weight diblock copolymer, PS−PMMA diblock copolymer of $M_w = 1.53 \times 10^6$, in mixed selective solvents of benzene and *p*-cymene through dynamic and static light scattering (DLS and SLS) and intrinsic viscosity experiments. Benzene was a good solvent for both PS and PMMA,

* To whom correspondence should be addressed.

† Present address: Toyobo Research Center, Toyobo Co., Ltd., 1−1 Katata 2-chome, Ohtsu, Siga, 520-0243, Japan.

10.1021/jp991319c CCC: $18.00
Published on Web 09/24/1999

TABLE 1: The Specific Refractive Index Increments $\nu = (dn/dc)$ for Homopolymers [PS (≡S) and PMMA (≡M)] and PS−PMMA Diblock Copolymer [BMM313 (≡SM), 38.5 wt %PS] in Single Solvents [Benzene (≡bz) and *p*-cymene (≡pcy)] and a Mixed Solvent ϕ_1 (bz/pcy=40/60 v/v) at 30.0 °C[a]

polymer/solvent	notation	dn/dc exptl.	dn/dc calc.[b]	preferential adsorption
PS/bz	$(\nu)_{S,bz}$	0.1105[c]	0.1104	
PMMA/bz	$(\nu)_{M,bz}$	0.0003	0.0002	
BMM313/bz	$(\nu)_{SM,bz}$	0.0427[c]	0.04273	not obsd
PS/pcy	$(\nu)_{S,pcy}$	0.1195	0.1202	
PMMA/pcy	$(\nu)_{M,pcy}$	ppt[d]	0.0044	
BMM313/pcy	$(\nu)_{SM,pcy}$	ppt[d]	0.04898	
PS/bz/pcy(4/6)	$(\nu)_{S,4/6}$	0.1130	0.1163	not obsd
PMMA/bz/pcy(4/6)	$(\nu)_{M,4/6}$	ppt[d]	0.0028	
BMMA313/bz/pcy(4/6)	$(\nu)_{SM,4/6}$	0.06863	0.04648	obsd

[a] For example, $(\nu)_{SM,4/6}$ denotes the specific refractive index increment of BMM313 in the mixed solvent of bz/pcy=40/60 v/v. [b] For the method of calculation, see the text. [c] Our previous data.[9] [d] The value cannot be measured because the polymer precipitates in the solvent.

while *p*-cymene was selective, or good for PS but poor/precipitant for PMMA. The additional situation, i.e., both solvents presented zero in the specific refractive index increments to PMMA but gave a small definite difference in the refractive indices for a 488-nm line at 30.0 °C, was extremely effective to the present study. We successfully proceeded to detect the scattered light only from the PS subchain and to grasp clear understanding on the dynamics of diblock copolymer in mixed selective solvents, where the solution contained the single block copolymer (i.e., unimer) and the intermolecular micelle of uniform size.

Experimental Section

Polymer Samples and Solvents. An anionically prepared polystyrene(PS)-*block*-poly(methyl methacrylate)(PMMA) copolymer, coded as BMM313, was used for the present study, which was characterized previously[9] as weight-average molecular weight $M_w = 1.53 \times 10^6$, PS content = 38.5 wt %, and $M_w/M_n = 1.01$. A homo-PS, designated as RS13, was used, which was a precursor of molecular weight exactly the same as that of the PS subchain in BMM313, $M_w = 0.589 \times 10^6$.[9] Benzene (BZ) and *p*-cymene (PCY) were chosen as solvents for the present mixed solvent system because BZ was a good solvent for both PS and PMMA, whereas PCY was a selective solvent, good for PS but poor/precipitant for PMMA. Moreover, BZ and PCY were both practically isorefractive to PMMA for a 488-nm line at 30 °C, i.e., the specific refractive index increments were extremely close to zero, 0.0003 and 0.0044, respectively, for PMMA, although the refractive indices of both solvents were slightly different from each other, as described below and shown in Table 1. The PMMA subchain was thus masked optically in the present system. PCY was purified by fractional distillation of the extra-pure reagent *p*-cymene (Nacalai tesque) under the N_2 atmosphere at 20 mmHg, the boiling point of collected fractions being 62 °C. BZ was prepared specially of the spectro-grade (Nacalai tesque). The purity of PCY and BZ was ascertained by their refractive indices, n_0, measured at three wavelengths of sodium D (589-nm) and of mercury (436-, 546-nm) lines on a Pulfrich refractometer (Shimadzu) at 30.0 °C. The results, for example, $n_{0,D}^{30}$ (pcy) = 1.48601 and $n_{0,D}^{30}$ (bz) = 1.49463, compared well with the literature values 1.4861 and 1.49470, respectively.[20] The refractive indices of PCY and BZ at 488 nm were obtained by interpolating the experimental values at three wavelengths to a 488 nm, with the result that $n_{0,488}^{30}$ (pcy) = 1.49580 and $n_{0,488}^{30}$ (bz) = 1.50614. This result shows that PCY and BZ are not strictly isorefractive to each other and that preferential adsorption will be observed. With the same procedure, the refractive indices of mixed PCY/BZ solvents were also determined at variety of the volume fractions of BZ, ϕ_{bz}. The values at 488 nm, n_0, were then found to be represented precisely by the relation

$$1/n_0 = \phi_{bz}/n_{0,bz} + \phi_{pcy}/n_{0,pcy} \qquad \phi_{bz} + \phi_{pcy} = 1 \qquad (1)$$

Here $n_{0,bz}$ and $n_{0,pcy}$ are the refractive indices of pure BZ and PCY at 488 nm, respectively.

Preparation of Mixed Solvents and Polymer Solutions. Mixed solvents of ϕ_{bz} were prepared by mixing two solvents by volume, where ϕ_{bz} was determined by using an equation expressed in terms of the weight of solvent, W_{bz} and W_{pcy}, as

$$\phi_{bz} = (W_{bz}/\rho_{bz})/(W_{pcy}/\rho_{pcy} + W_{bz}/\rho_{bz}) \qquad (2)$$

The density of a given mixed solvent ρ is expressed by

$$\rho = \phi_{pcy}\rho_{pcy} + \phi_{bz}\rho_{bz} \qquad (3)$$

with ρ_{pcy} and ρ_{bz} being the density of PCY and BZ, respectively; $\rho_{pcy} = 0.84930$ gcm^{-3} and $\rho_{bz} = 0.86845$ gcm^{-3} at 30.0 °C.

The viscosities η of mixed solvents and of pure solvents were determined at 30.0 °C by measuring the flow times t in a specified viscometer designed so that the relation $\eta = A\rho(t - B/t)$ should be reduced to a simple form $\eta = A\rho t$ without a kinetic energy correction. Distilled water was used for reference at 30.0 °C. The result of η at a given ϕ_{pcy} was well expressed by Kurata's expression[21]

$$(\eta - x_{bz}\phi_{bz}\eta_{bz})/x_{pcy}\phi_{pcy} = \eta_{pcy} + 2(x_{bz}\phi_{bz}/x_{pcy}\phi_{pcy})^{1/2}\phi_{bz}\,\eta_{bz-pcy} \qquad (4)$$

where $\eta_{pcy} = 0.7520$cp, $\eta_{bz} = 0.5621$cp, and $\eta_{bz-pcy} = 0.6366$cp at 30.0 °C with x_{pcy} (= W_{pcy}/M_{pcy}) the molar fraction of PCY and M_{pcy} the molecular weight of PCY, 134.2.

The original polymer solutions of mixed solvent fractions $0 < \phi_{pcy} \leq 0.60$ were prepared as follows. The weighed amounts of the freeze-dried BMM313 and the mixed solvent of ϕ_{pcy} were mixed in a flask, sealed under N_2 atmosphere, and heated at ca. 35 °C for a few days with intermittent stirring until homogeneous clear solutions appeared. The polymer mass concentration, c_0, of the fraction ϕ_{bz} was calculated from the equation

$$c_0 = (W/W_{solv})(\phi_{pcy}\rho_{pcy} + \phi_{bz}\rho_{bz}) \qquad (5)$$

with W and W_{solv} the weights of the polymer sample and of the mixed solvent, respectively. The solutions thus obtained were heated again for more than 24 h at ca. 35 °C. The same procedure failed to prepare a solution of $\phi_{pcy} = 0.70$ because BMM313 never dissolved in this mixed solvent. Therefore, the weighed amounts of BMM313 were first dissolved completely in the desired amounts of BZ and then PCY was added drop by drop into the BZ solution to attain $\phi_{pcy} = 0.70$ with continuous stirring of the solution at 30 °C, resulting in a clear solution. The solution was then heated for more than 24 h at ca. 35 °C.

Dynamic Light Scattering. Solutions of five different concentrations of a mixed solvent fraction $\phi_{bz} = 0.40$ were prepared by directly filtering the suitable amounts of the original solution and the mixed solvent of $\phi_{bz} = 0.40$ into an optically cleaned light scattering cell through 0.5 and 0.2 μm Millipore

filters, respectively. They were left for a few days at ca. 35 °C. The solutions thus prepared were of $c = (0.341-4.55) \times 10^{-3}$ gcm^{-3}, which correspond to $0.07c^*$ to $0.94c^*$, with c^* being the overlapping polymer mass concentration. The normalized intensity time correlation functions $A(t)$ were measured by the homodyne method at 30.0 °C for the V_v component of a single-frequency 488-nm line emitted from an etalon-equipped 3W argon-ion laser (Spectra Physics). A laboratory-made time interval software correlator of 512 channels (with equally spaced delay times) was suitably used for the present purpose because the correlator was extremely sensitive to weak scattering light. The $A(t)$ profiles obtained at $\theta = 10°-150°$ were analyzed through the histogram method. The details were given elsewhere,[9,22] but a brief description will be helpful for the later discussion. The electric field time correlation function $g^{(1)}(t)$ defined by $A(t) = 1+\beta|g^{(1)}(t)|^2+\delta$ is expressed in terms of the decay rate Γ as

$$g^{(1)}(t) = \int_0^\infty G(\Gamma) \exp(-\Gamma t)\, d\Gamma \quad (6)$$

Here $G(\Gamma)$, given by $G(\Gamma) = \sum_k G_k(\Gamma)$, represents the decay rate distribution that is composed of k pieces of histogram $G_k(\Gamma)$. β (≤ 1) is a measure of coherency in the apparatus and δ ($\sim 10^{-3}$) is the baseline correction. The mean decay rate Γ_k and the mean fractional amplitude f_k for the kth histogram (or mode) were calculated with the distribution $G_k(\Gamma)$ as

$$\Gamma_k = \int_k \Gamma G_k(\Gamma) d\Gamma / f_k,\ f_k = \int_k G_k(\Gamma) d\Gamma,\ \sum_k f_k = 1 \quad (7)$$

with $\int_k$ the integration over solely the Γ range limited for the kth histogram. The first cumulant, or the overall effective decay rate, Γ_e was obtained from

$$\Gamma_e = \int_o^\infty \Gamma G(\Gamma) d\Gamma = \sum_k f_k \Gamma_k \quad (8)$$

It should be noted that Γ_e represents all the motions existing in the system investigated.

Static Light Scattering. Solutions of $\phi_{bz} = 0.40$ with five different concentrations, $c = (0.787-3.93) \times 10^{-3}$ gcm^{-3}, were prepared and stored under the same procedures and conditions as described above. The scattered intensity measurements for each solution were made at 30.0 °C and at $\theta = 20°-150°$ for the V_v component of a 488-nm line on a DLS/SLS-500 spectrometer/goniometer (ALV). The dependence of the reciprocal reduced scattered light intensity $Kc/R(\theta)$ on the angle and the concentration were analyzed with the Berry plot. Here $R(\theta)$ is the Rayleigh ratio and K is the optical constant given by $K = 4\pi^2 n_0^2 (dn/dc)^2/\lambda_0^4 N_A$, with n_0 the refractive index of the mixed solvent and dn/dc ($= \nu$) the specific refractive index increment of the solution at $\lambda_0 = 488$ nm.

Specific Refractive Index Increment. The specific refractive index increments dn/dc for BMM313 and RS13 in a mixed solvent of $\phi_{bz} = 0.40$ were measured on the differential refractometer DRM-1021 (Otsuka Electronics) at 30.0 °C for a 488-nm line. Aqueous KCl solutions were used for the standard calibration of the apparatus. The results of dn/dc are summarized in Table 1. Here, the expression $(\nu)_{SM,4/6} = 0.06863$, for example, represents the value for BMM313 (suffix SM) and the suffix 4/6 refers to the volume fraction of BZ/PCY. The dn/dc of PMMA in BZ was measurable, $(\nu)_{M,bz} = 0.0003$, while that of PMMA in PCY and in a mixed solvent of $\phi_{bz} = 0.40$ were calculated to be $(\nu)_{M,pcy} = 0.0044$ and $(\nu)_{M,4/6} = 0.0028$, respectively, since PMMA precipitated in these solvents. The dn/dc of $(\nu)_{M,bz} = 0.0003$ and $(\nu)_{M,pcy} = 0.0044$, both being extremely near to zero, ascertains that the PMMA part of the present block copolymer is masked optically in BZ and PCY to within the accuracy of $\nu = \pm 0.004$. In contrast to this, PS gave the finite and large values of dn/dc. Moreover, the values of $n_{0,488} = 1.49857$, $\eta = 0.6393$cp, and $\rho = 0.85696$ gcm^{-3} were obtained for the mixed solvent of $\phi_{bz} = 0.40$ at 30.0 °C.

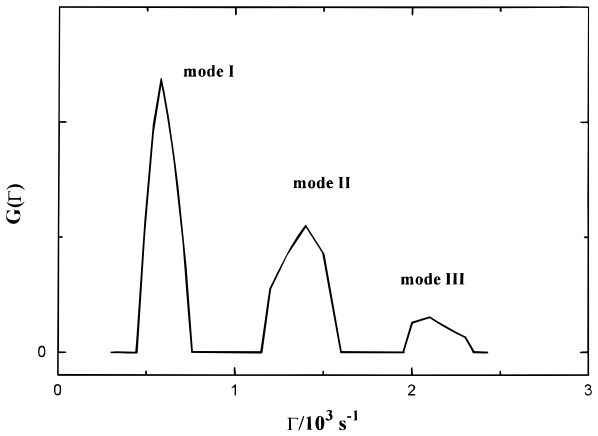

Figure 1. The decay rate distribution $G(\Gamma)$ plotted against Γ for BMM313 in a mixed solvent of benzene/*p*-cymene, $\phi_{bz} = 0.40$, at 30.0 °C. The polymer mass concentration c is 2.36×10^{-3} gcm^{-3} and the scattering angle θ is 90°. Three decay modes, which are denoted as modes I, II, and III in the increasing order of Γ, coexist with each other in the solution. Modes I and II represent the diffusion of micelles and of unimers, respectively, and mode III represents the internal motions of micelles.

Intrinsic Viscosity. BMM313 solutions of different mixed solvent fractions ($\phi_{pcy} = 0-0.70$) were measured on the Ubbelohde type of a capillary viscometer at 30.0 °C. The shear rate $\dot{\gamma}$ was calculated by $\dot{\gamma} = H\rho g a/2\eta_{soln} L$, with the capillary radius $a = 0.022$ cm, the liquid height $H = 14.8$ cm, the capillary length $L = 12.7$ cm, and the acceleration of gravity g. The solution was filtered through a 0.5 μm pore size filter (Millipore) just prior to use. For PS, two solutions of RS13 of $\phi_{pcy} = 0$ and 0.60 were also measured, where the solution was filtered through a 0.2 μm pore size filter. The kinetic energy correction was neglected since the flow time was more than 130s for solvents. The intrinsic viscosity $[\eta]$ was determined by three methods: $\eta_{sp}/c = [\eta] + k'[\eta]^2 c + ...$; $\ln\eta_r/c = [\eta] - \beta[\eta]^2 c + ...$ ($\beta = 0.5$-k'); and $\eta_{sp}/c = [\eta] + k'[\eta]\eta_{sp} + ...$, where η_{sp}, η_r, and k' are the specific and the relative viscosities and the Huggins constant, respectively.

Results

DLS Characteristics. $A(t)$ for BMM313 solutions of $\phi_{bz} = 0.40$ gave two modes of motions at $\theta \leq 60°$, and three modes at $\theta \geq 90°$, irrespective of polymer concentrations. Figure 1 is an example of the decay rate distribution $G(\Gamma)$ for the solution of $c = 2.36 \times 10^{-3}$ gcm^{-3} at $\theta = 90°$. $G(\Gamma)$ is separated into three discrete peaks with the variance as small as 0.01−0.03, and each peak was designated as modes I, II, and III in the increasing order of Γ. The corresponding mean decay rates, Γ_I, Γ_{II}, and Γ_{III}, and the fractional amplitude, f_I, f_{II}, and f_{III}, were obtained by taking the average only over the respective peak. Figure 2 exemplifies the concentration dependence of $\Gamma_k/\sin^2(\theta/2)$ at $\theta = 10°-150°$ for these modes. As described above, modes I and II appear at every θ of 10°−150° (six symbols), whereas mode III appears only at $\theta = 90°-150°$ (three symbols; ∇, +, ○). For each mode, $\Gamma_k/\sin^2(\theta/2)$ at a given θ is found to be constant, independent of c over all c measured. This constancy confirms that the size for each mode of motion is not affected by c. Hence, the infinite dilution value $[\Gamma_k/\sin^2(\theta/$

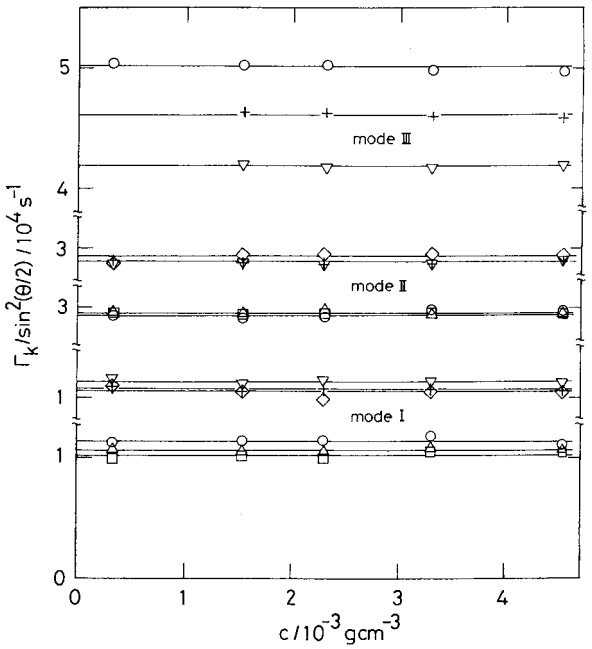

Figure 2. Concentration dependence of the decay rate $\Gamma_k/\sin^2(\theta/2)$ for mode k (k = I, II, III) at six scattering angles $\theta = 10-150°$ for BMM313 in a mixed solvent of benzene/*p*-cymene, $\phi_{bz} = 0.40$, at 30.0 °C: $\theta = 10°$(□); 30°(◇); 60°(△); 90°(▽); 120°(+); 150°(○).

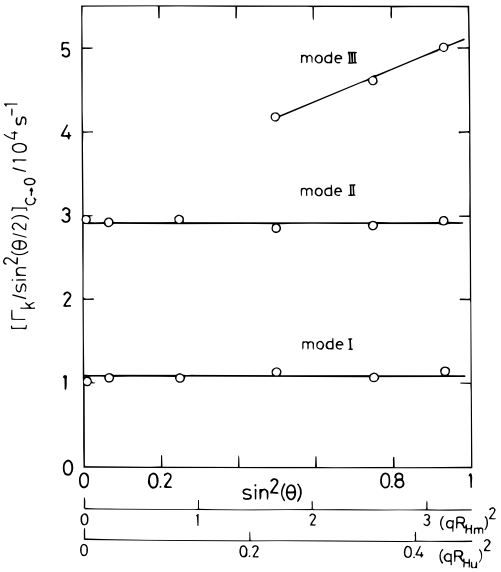

Figure 3. Angular dependence of the decay rate at infinite dilution $[\Gamma_k/\sin^2(\theta/2)]_{c=0}$ for BMM313 in a mixed solvent of benzene/*p*-cymene, $\phi_{bz} = 0.40$, at 30.0 °C. The abscissa is expressed in terms of $\sin^2(\theta/2)$, $(qR_{Hm})^2$, or $(qR_{Hu})^2$ with R_{Hm} and R_{Hu} the hydrodynamic radii of the micelle and unimer, respectively. Mode I is the diffusion of the micelle, mode II is the diffusion of the unimer, and mode III is the intramicellar motions.

2)]$_{c=0}$ at a given θ was estimated by averaging $\Gamma_k/\sin^2(\theta/2)$ over five different c. The obtained $[\Gamma_k/\sin^2(\theta/2)]_{c=0}$ is plotted in Figure 3 as a function of $\sin^2(\theta/2)$ for three modes. The value is independent of θ for modes I and II, but depends on θ for mode III. Thus, the former two modes are the translational diffusion motion, whereas the latter is the relaxation motions of the chain, as ascertained below. The diffusion coefficient D_k for the two modes was evaluated from the relation $D_k = \Gamma_k/q^2 = [\Gamma_k/\sin^2(\theta/2)]_{c=0}/(4\pi n_0/\lambda_0)^2$ to be $D_I = 7.26 \times 10^{-8}$ and $D_{II} = 1.96 \times 10^{-7}$ cm^{2}s^{-1} (for details, see Appendix). Since $D_I < D_{II}$, mode I represents a diffusion motion much slower than

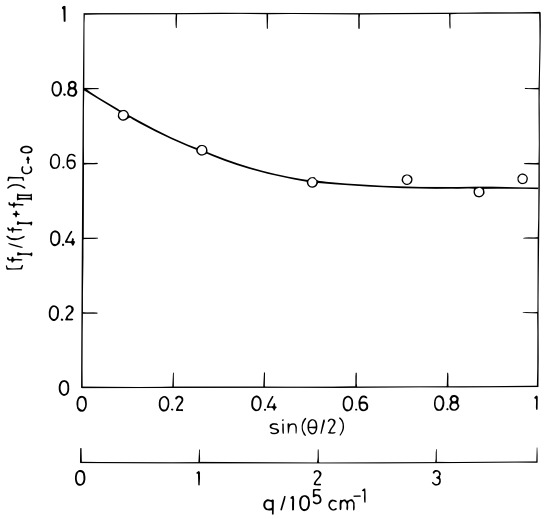

Figure 4. Fractional amplitude of the diffusion mode of micelles f_I to the total (= micelle and unimer) diffusion motions $f_I + f_{II}$ at infinite dilution, $[f_I/(f_I + f_{II})]_{c=0}$, plotted against $\sin(\theta/2)$ or q for BMM313 in a mixed solvent of benzene/*p*-cymene, $\phi_{bz} = 0.40$, at 30.0 °C.

that of mode II, and is assigned to the micellar center-of-mass diffusion. Mode II is the diffusion of a single BMM313 copolymer, or the unimer particle. The small variance of mode I, 0.01, ascertains the sharpness of the Γ distributions of micelles (see Figure 1) and confirms that the size of the present micelle is almost uniform. Thus, the unimer and the micellar particles of uniform size coexist in the mixed solvent of $\phi_{bz} = 0.40$. Under the condition that PMMA was masked optically in this solvent, the hydrodynamic radii of the micelle and the unimer, R_{Hm} and R_{Hu}, were evaluated to be $R_{Hm} = 47.8$ nm and $R_{Hu} = 17.7$ nm (see below). Here the Stokes−Einstein relation $R_{Hk} = k_BT/6\pi\eta D_k$ was used with k_B and T, the Boltzmann constant and the absolute temperature, respectively. The micelle size is 2.7 times larger than the unimer size, or $R_{Hu}/R_{Hm} = 0.370$. It should be noted that the obtained D_I, D_{II}, R_{Hm}, and R_{Hu} are not the apparent but the true values for the unimer and micelle, of which sizes are of substantially monodisperse (see eqs A19−A23 in Appendix).

According to Figures 2 and 3, the concentration-dependent coefficient k_D, which is defined in the expression

$$D(c) = D_0(1 + k_D c + ...) \qquad \text{(modes I and II)} \qquad (9)$$

and represents the hydrodynamic second virial coefficients, is equal to zero for both unimers and micelles. This fact means that, in the present solution, the interparticle hydrodynamic interactions disappear and the particles are in a stable state hydrodynamically.

In Figure 3, we express the abscissa in terms of the reduced micelle size $(qR_{Hm})^2$, together with $\sin^2(\theta/2)$. Mode III, which depends on θ, is then found to appear only at $(qR_{Hm})^2 \geq 1.7$. This trend is quite similar to the case of flexible linear polymers in the intermediate region of $qR_H > 1$ where the internal modes of motions come to appear.[23] Hence, it is strongly suggested that mode III represents the intramicellar motions, and that the micelle structure may not be rigid but flabby in the dynamic sense.

In Figure 4 the amplitude ratio at infinite dilution $[f_I/(f_I + f_{II})]_{c=0}$ is plotted against q or $\sin(\theta/2)$. Here, f_I and f_{II} are the fractional amplitudes of the translational diffusions for micelles and unimers, respectively, as assigned already. As shown in the Appendix, f_I is proportional to $P_m(\theta)\gamma_m M_m$ at small q with

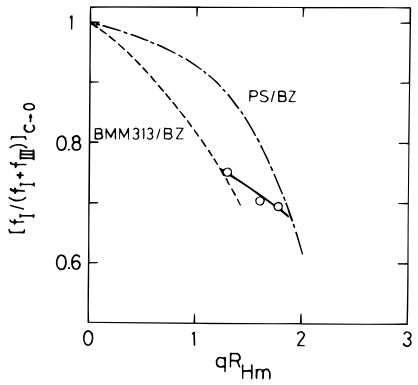

Figure 5. Fractional amplitude of the diffusion motion of micelle f_I to the total motions of micelle $f_I + f_{III}$ at infinite dilution, $[f_I/(f_I + f_{III})]_{c=0}$, plotted against qR_{Hm} for BMM313 in a mixed solvent of benzene/*p*-cymene, $\phi_{bz} = 0.40$, at 30.0 °C (unfilled circles). The chain line represents the results for homo-PS in benzene at 30.0 °C[24] and the broken line for the present diblock copolymer BMM313 in benzene at 30.0 °C.[9] For both cases, R_{Hm} represents the hydrodynamic radius of PS and BMM313 chains in benzene.

P_m, γ_m, and M_m being the particle scattering factor, weight fraction, and molecular weight of the micellar particle, respectively. Therefore, the ratio $f_I/(f_I + f_{II})$ is the fraction of the micellar diffusion motion to the total diffusion motions that exist in the system. Figure 4 then reveals that the fraction of the micellar diffusion decreases with q and approaches to a constant at $q > 3 \times 10^5$ cm^{-1}. Inversely, at $q \to 0$, the fraction becomes 0.80, which gives that $f_I(q=0)/f_{II}(q=0) = P_m(0)\gamma_m M_m/P_u(0)\gamma_u M_u = \gamma_m M_m/\gamma_u M_u = 0.80/0.20 = 4.0$. Here the subscript u denotes the unimer particle.

In Figure 5 the amplitude ratio estimated from modes I and III at infinite dilution, $[f_I/(f_I + f_{III})]_{c=0}$, is plotted against qR_{Hm} by three unfilled circles. This ratio represents the micellar diffusion relative to the total micellar motions (see Appendix). It ranges from 0.75 to 0.70. Thus, the internal motions of the micelle, which can be estimated from $1- [f_I/(f_I + f_{III})]_{c=0}$, become 0.25−0.30. This value is much larger than that for PS homopolymers in BZ (the chain curve)[24] because the three data points are located much below the chain curve at $1.3 < qR_{Hm} < 1.8$, but is comparable to or less than that of the present copolymer BMM313 in pure BZ (the broken curve)[9] at the same qR_{Hm}. Such a high degree of flexibility inside the micelle certifies again the loose association state characteristic of the present micelle.

SLS Characteristics. The reciprocal reduced scattered intensity $Kc/R(\theta)$ for all of the solutions measured is plotted against q^2 in Figure 6. For six curves, the polymer mass concentration c decreases from 3.93×10^{-3} gcm^{-3} to zero ($c \to 0$), from top to bottom. The curve at $c \to 0$ was obtained by the linear extrapolation of the values at finite concentration to infinite dilution at a given θ. Given that the five curves at finite c are shifted by some constant B multiplied by c to the right-hand side in the abscissa, or changing the abscissa from q^2 to $q^2 + Bc$, we can obtain the Zimm plot in place of Figure 6. There is no essential difference between the Zimm plot and Figure 6, and so the former is not shown here. In Figure 6, each $Kc/R(\theta)$ increases linearly with q^2 at lower q^2, but shows sigmoidal behavior at higher q^2, which would result from the micellar structure. In Figure 7 the Berry plots are shown, where the reciprocal square-root values at the infinite dilution $[Kc/R(\theta)]_{c=0}^{1/2}$ and at the zero scattering angle $[Kc/R(\theta=0)]^{1/2}$ are plotted against q^2 and against c, respectively, by unfilled and filled circles. From the initial slopes and the intercepts in these plots, we obtained that the apparent radius of gyration $R_G^* = 5.36 \times 10^{-6}$ cm, the apparent molecular weight $M^* = 1.23 \times 10^6$, and the apparent second virial coefficient $A_2^* = 1.23 \times 10^{-4}$ cm^3 mol g^{-2}.

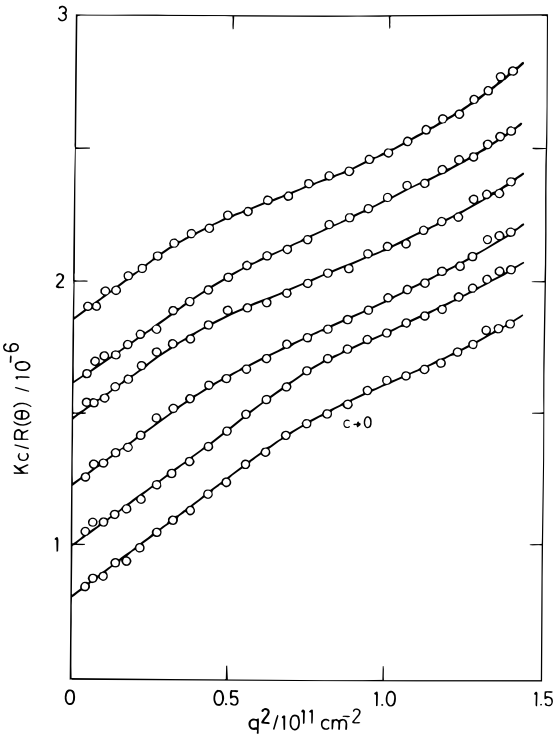

Figure 6. The modified Zimm plots, or the angular dependence of the reciprocal reduced scattered intensity $Kc/R(\theta)$ at five different polymer mass concentrations c and at infinite dilution for BMM313 in a mixed solvent of benzene/*p*-cymene, $\phi_{bz} = 0.40$, at 30.0 °C. Here, c (10^{-3} gcm^{-3}) is 3.93, 3.15, 2.36, 1.57, 0.787, and 0, from top to bottom.

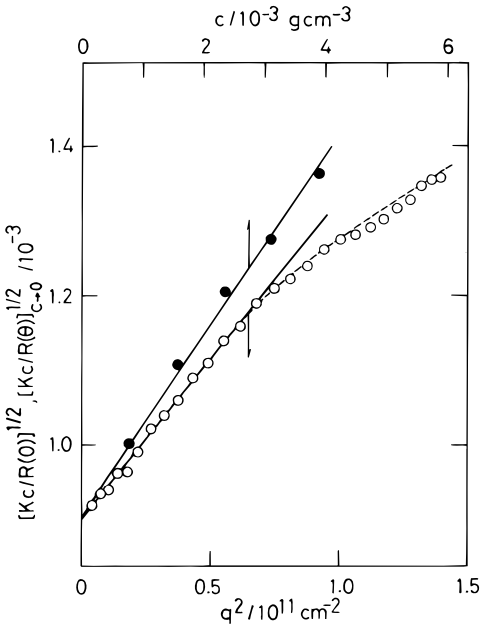

Figure 7. Berry plots of the infinite dilution values $[Kc/R(\theta)]_{c=0}^{1/2}$ against q^2 (unfilled circles) and the zero angle values $[Kc/R(\theta=0)]^{1/2}$ against c (filled circles) for BMM313 in a mixed solvent of benzene/*p*-cymene, $\phi_{bz} = 0.40$, at 30.0 °C. The broken line represents the theoretical values calculated for the mixture of micelle and unimer, both of which are of the hollow Gaussian chain shell structure (for details, see the text).

The A_2^* of positive and usual magnitude indicates that the present solution of $\phi_{bz} = 0.40$ is not so favorable for the block copolymer to associate tightly. This suggests that the micelle

TABLE 2: Characteristics of Micelles and Unimers for PS−PMMA Diblock Copolymer (BMM313) in a Mixed Selective Solvent of Benzene/*p*-Cymene = 40/60(v/v), i.e., $\phi_{bz} = 0.40$, at 30.0 °C[a]

	ϕ_{bz}=0.40				ϕ_{bz}=1.0[b]	
	micelle	mixture	block copolymer (unimer)	homo-PS (precursor)	block copolymer (single chain)	homo-PS[a] (precursor)
w	0.599		0.401		1.0	
$M_w \times 10^{-6}$	4.60		1.53	0.589	1.53	0.589
z	3		1		1	(precursor)
R_H, nm	47.8		17.7		35.0	36.2
R_G, nm	58.9		21.8[c]		41.0	24.8
R_G/R_H	1.23		1.23		1.17	1.46
$R_{H,\phi bz=0.4}/R_{H,bz}$			0.506			
$R_{G,\phi bz=0.4}/R_{G,bz}$			0.532			
k_D, cm^3g^{-1}	0		0		113	118
$A_2^* \times 10^4$,cm^3molg^{-2}		1.23			1.67	3.56
$[\eta]$, cm^3g^{-1}			210	153	411	184
R_V, nm			37.1	24.3	46.3	25.8
R_H/R_V,			0.477		0.756	1.40
$R_{V,\phi bz=0.4}/R_{V,bz}$			0.801	0.941		
	The Hollow Gaussian Chain Shell Model[c]					
$2<S^2>_{SG}^{1/2}$,nm	54.0[c]		20.0[c]			
$r_c/2<S^2>_{SG}^{1/2}$		0.50[c]				
R_{Gu}/R_{Gm}		0.370[c]				

[a] Homo-PS means the precursor of BMM313, the molecular weight being equal to that of the PS part of BMM313. [b] Our previous data for BMM313 in benzene at 30.0 °C.[9] [c] Theoretical values calculated by the hollow Gaussian chain shell model.

TABLE 3: Viscosity Results of PS−PMMA Diblock Copolymer (BMM313) and Homo-PS (RS13, the precursor of BMM313) in Mixed Selective Solvents of Benzene/*p*-Cymene at 30.0 °C[a]

	BMM313		RS13	
ϕ_{bz},[b] v/v	$[\eta]$, cm^3g^{-1}	k'	$[\eta]$, cm^3g^{-1}	k'
1.00	411	0.308	184	0.320
0.90	391	0.338		
0.80	366	0.304		
0.70	338	0.316		
0.60	302	0.342		
0.50	259	0.351		
0.40	210	0.340	153	0.336
0.30	112	0.475		

[a] The shear rate $\dot{\gamma}$ was 1700−2000 s^{-1} at infinite dilution. [b] $\phi_{pcy} + \phi_{bz} = 1$.

would be formed under weak segregation conditions, that is, the birth of the micelle core would be followed by the gentle growth of the micelle, resulting in a micelle of thermodynamically equilibrium size. This situation is consistent with the experimental fact that the hydrodynamic size of the micelle R_{Hm} does not depend on the solution concentrations, as already shown in Figures 2 and 3.

Intrinsic Viscosity. The $[\eta]$ and k' values observed for solutions of BMM313 and of RS13 (the PS part of BMM313) in mixed solvents are summarized as a function of ϕ_{bz} in Table 3. The shear rate $\dot{\gamma}$ exerted on solute molecules was in the range of 1700−2000 s^{-1} at infinite dilution. As ϕ_{bz} decreases, $[\eta]$ of RS13 decreases from 184 cm^3g^{-1} in pure BZ to 153 cm^3g^{-1} at $\phi_{bz} = 0.40$, the decrease being by 17%. This means that the PS part of BMM313 does not so shrink as the solvent quality decreases. On the other hand, $[\eta]$ for BMM313 solution, whose PS and PMMA parts expanded well in pure BZ,[9] decreases sharply with decreasing ϕ_{bz}, and it becomes one half at $\phi_{bz} = 0.40$ and one quarter at $\phi_{bz} = 0.30$, the latter being much smaller than $[\eta]$ for RS13 at $\phi_{bz} = 0.40$. This behavior of BMM313 may reflect a strong shrinkage of the PMMA part, followed by the intermolecular micelle core formation. If the micelle would exist solely, the decrease in $[\eta]$ might indicate an increase in the density of the micelle corona, which is composed of the PS part, and the situation could be expressed by a relation that $[\eta] = P_{sh}/d_m$[23,14] with P_{sh} the shape factor and d_m the density of the micelle. As shown already, however, the present solution of $\phi_{bz} \geq 0.40$ was composed not of micelles alone but of mixture of unimers and micelles. The situation is not so simple as assumed above.

Discussion

Preferential Adsorption. As mentioned in the Experimental Section, the refractive indices of BZ and PCY are not exactly the same to each other, which situation was intended in the present study. Hence, this difference in n in the two solvents gives information on the preferential adsorption.[25−28] Let ν_{A1} be the specific refractive index increment of homopolymer A in single solvent 1; $\nu_{A1} = (dn/dc)_{A1}$. Since the additivity of polarizabilities is well founded for copolymers and for mixed solvents,[25−28] the $(dn/dc)_{AB\phi1}$ for the quadruple combination of A−B diblock copolymer (the weight fraction of the A part is w_A) in the mixed solvent of 1 and 2 (the volume fraction of good solvent 1 is ϕ_1) is expected to be given by

$$\nu_{AB\phi1} \equiv (dn/dc)_{AB\phi1} = \sum_{j=A,B;k=1,2} w_j \nu_{0,jk} \phi_k \qquad (10)$$

if the preferential adsorption does not occur (see Appendix). Here the suffix 0 in $\nu_{0,jk}\phi_k$ denotes that the ν value is calculated under no preferential adsorption. A similar relation is also expected for triple combinations such as one homopolymer in mixed solvents and as one copolymer in single solvent. The ν values calculated for the present system in this expectation are summarized in Table 1, together with the corresponding experimental values. Agreement between experiments and calculations is very good in the cases of triple combinations of A−B copolymer in single solvent, BMM313/bz, and homo-A in mixed solvent, PS/bz/pcy(4/6). Thus, no preferential adsorption of BZ or PCY to PS or PMMA was observed. The same situation holds for the case where precipitation occurs, i.e., BMMA313/pcy and PMMA/bz/pcy(4/6). The Gladstone−Dale relation, which is referred to the simple combinations of one homopolymer in single solvent, held also for PS/bz, PMMA/bz, PS/pcy, and will hold for PMMA/pcy, in which the precipitation occurs. Thus, exception was observed only for the

full combination of A−B copolymer in mixed solvents, BMM313/bz/pcy(4/6). The difference between experiments and calculations, 0.06863 and 0.04648 (Table 1), is out of errors, and it indicates a strong preferential adsorption. Since PCY is precipitant to PMMA, it could be considered that PCY would be excluded from the vicinity of PMMA. This change, which is expressed by the preferential adsorption parameter of PCY to PMMA, $\alpha_{M,pcy}$, affects the other three parameters, $\alpha_{M,bz}$ (BZ to PMMA), $\alpha_{S,bz}$ (BZ to PS), and $\alpha_{S,pcy}$ (PCY to PS). All of these parameters are related to each other under the assumption that no volume change occurs by the preferential adsorption (eq A10)

$$\alpha_{S,bz} + \alpha_{M,bz} + \alpha_{S,pcy} + \alpha_{M,pcy} = 0 \tag{11}$$

It should be noted here that, as revealed in DLS characteristics, the present solution contains a single copolymer (unimer) and its micelle. Hereafter, we assume the same state of preferential adsorption in the unimer and the micelle, i.e., they have the similarity in the structure and in the dn/dc. Under this condition, the effect of preferential adsorption on the data reduction is taken into consideration in the following discussions. Refer to the Appendix for details.

Characterization of Mixture of Unimer and Micelle. In the present system, PMMA is practically isorefractive to BZ and PCY, that is, $\nu_{M,bz} = \nu_{M,pcy} \cong 0$ (± 0.004) as shown in Table 1. As mentioned above and in the Appendix, we assume that (i) the preferential adsorption induces no change in the total volume of solvents and (ii) both unimers and micelles are in the same preferential adsorption state/structure. Then, the apparent molecular weight M^* of the mixture in the mixed solvent of $\phi_1 = 0.40$ is written from eqs A12−A15 as

$$M^* = (\nu_{\phi 1}/\nu)^2 (\gamma_u M_u + \gamma_m M_m) \tag{12}$$

$$\nu_{\phi 1} \equiv \nu_u = \nu_m = (\mathrm{d}n/\mathrm{d}c)_{0,\phi 1}[1 + (\alpha_{S,bs} + \alpha_{M,bz})\{(\mathrm{d}n_0/\mathrm{d}\phi_1)/(\mathrm{d}n/\mathrm{d}c)_{0,\phi 1}\}] \tag{13}$$

where $\mathrm{d}n_0/\mathrm{d}\phi_1$ is the variation of the refractive index of mixed solvents with the composition and $(\mathrm{d}n/\mathrm{d}c)_{0,\phi 1}$ is the specific refractive index increment in the solution of a mixed content ϕ_1 with no preferential adsorption. The former was obtained from eq 1 as a definite nonzero value, $\mathrm{d}n_0/\mathrm{d}\phi_1 = (n_{0,pcy}^{-1} + n_{0,bz}^{-1})(n_{0,\phi 1})^2 = 0.0103$. Inserting experimental and/or calculated values of $\nu = \nu_{SM,4/6} = 0.06863$, $(\mathrm{d}n/\mathrm{d}c)_{0,\phi 1} = \nu_{0,SM,4/6} = 0.04648$ (Table 1), and $M^* = 1.23 \times 10^6$ into eq 12, we have

$$2.68 \times 10^6 = (\gamma_u M_u + \gamma_m M_m)[1 + 0.221(\alpha_{S,bs} + \alpha_{M,bz})]^2 \tag{14}$$

where M_u ($= 1.53 \times 10^6$) and M_m are the weight-average molecular weights, and γ_u and γ_m are the weight fraction of unimer and micelle, respectively.

On the other hand, we have the results that $f_I(q{=}0)/f_{II}(q{=}0) = \gamma_m M_m/\gamma_u M_u = 4.0$ in the DLS experiments (Figure 4). Combining this relation with eq 14 gives information on the association number of micelle z ($= M_m/M_u$), the preferential adsorption parameter $\alpha_{S,bs}$, the weight fraction of unimer γ_m, and so on, provided that we have the third relation on these variables. We already know that the micelle is in a state of *loose* association, usually composed of small z. Therefore, we assume that $z = 3$, although verified later (see the section entitled *Micellar Structure*). Then, it follows that $\alpha_{S,bz} + \alpha_{M,bz} = -0.433$, together with the results that $\gamma_u = 3/7$, $\gamma_m = 4/7$, and $M_m = 4.60 \times 10^6$. The negative large value of $\alpha_{S,bz} + \alpha_{M,bz}$ means that the preferential adsorption not of BZ but of PCY occurs to the unimer/micelle particles. Since PCY is precipitant to the PMMA part, the preferential adsorption of a large amount of PCY should occur in the PS part. PCY excluded from the PMMA part is received in the PS part, and the total BZ composition in the PS and the PMMA parts is reduced considerably below the bulk value of no preferential adsorption. PMMA might construct the core part with a small amount of BZ. Moreover, it is interesting to note that the present value $\alpha_{S,pcy} + \alpha_{M,pcy} = -(\alpha_{S,bz} + \alpha_{M,bz}) = 0.433$ compares well to the case of PS in BZ/methanol(8/2) ($\alpha_{S,bz} = 0.405$), a typical polymer in a good (BZ)/precipitant(methanol) system.[27]

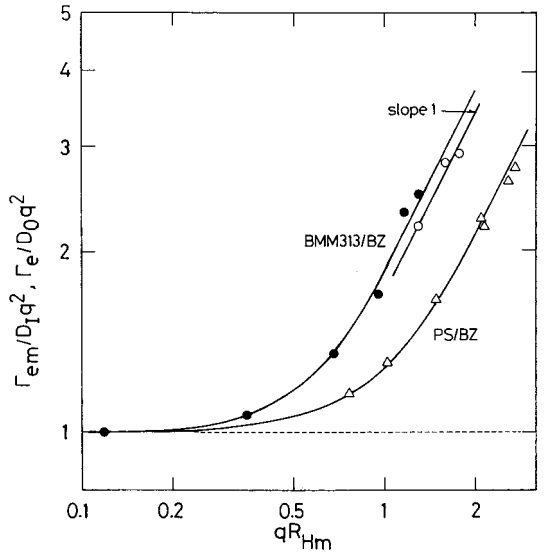

Figure 8. $\Gamma_{em}(\theta)/D_I q^2$, the universal ratio defined by the first cumulant relative to the diffusional decay rate, for the micelle of BMM313 in a mixed solvent of benzene/*p*-cymene at $\phi_{bz} = 0.40$ is plotted against qR_{Hm} (unfilled circles) at 30.0 °C. Other data represent the $\Gamma_e(\theta)/D_0 q^2$ vs qR_H plots for homo-PS in benzene at 30.0 °C[24] (△) and for BMM313 in benzene at 30.0 °C[9] (●).

Intramicellar Motions. The first cumulant of micelle, $\Gamma_{em}(\theta)$, is given from eq A19 as

$$\Gamma_{em}(\theta) = [f_I(\theta) + f_{III}(\theta)]\Gamma_m(\theta) = f_I(\theta)\Gamma_I(\theta) + f_{III}(\theta)\Gamma_{III}(\theta) \tag{15}$$

The second equation can be approved only for the present case (Figure 3) where the translational (mode I) and the internal (mode III) motions were observed simultaneously in the micelle at $\theta \geq 90°$. Thus, $f_I(\theta)\Gamma_I(\theta)$ and $f_{III}(\theta)\Gamma_{III}(\theta)$ represent the translational and the intramicellar motions, respectively. Since the experimental results show that $\Gamma_I(\theta)/q^2$ is independent of θ, which is the rigorous requirement to give the diffusion coefficient, we have the translational diffusion coefficient for the micelle, D_I. The universal ratio defined by $\Gamma_{em}(\theta)/D_I q^2$ for the micelle then becomes

$$\Gamma_{em}(\theta)/D_I q^2 = [f_I(\theta)\Gamma_I(\theta) + f_{III}(\theta)\Gamma_{III}(\theta)]/f_I(\theta)\Gamma_I(\theta) \tag{16}$$

With the experimental values of $f_I(\theta)$ and $f_{III}(\theta)$ at $\theta \geq 90°$, this ratio is plotted against qR_{Hm} in Figure 8 by unfilled circles. For reference, the universal ratios $\Gamma_e(\theta)/D_0 q^2$ for other systems are shown by filled circles (our previous data for single PS−PMMA diblock copolymer (BMM313) in benzene[9]) and by unfilled triangles (our data for homo-PS in benzene,[24] which is a typical example of linear flexible chains in good solvents). For the latter two cases, D_0 denotes the diffusion coefficient of

the corresponding polymers. The $\Gamma_{em}(\theta)/D_I q^2$ values in the mixed solvent are found to fall on a limiting line of slope 1 and show the nondraining q^3 dependency of Γ_{em}. This feature is similat to the internal motions of flexible linear chains at $qR_H > 1$ (the PS/BZ curve). However, it is very interesting that this limiting behavior appears around $qR_{Hm} = 1$, which locates in a fairly early stage of the intermediate region defined by $qR_{Hm} > 1$ and compares well to the line for a single BMM313 in BZ. The behavior of intramicellar motions presented here corresponds well to the intramicellar amplitude shown in Figure 5, where the amplitude of intramicellar motions, $1 - [f_I/(f_I + f_{III})]_{c=0}$, is revealed to be equal to or slightly smaller than that of the single copolymer (BMM313/BZ) but much larger than that of flexible linear chains (PS/BZ). Thus, the present micelle plays actively the internal modes of motions. These active intramicellar motions indicate that the present micelle retains flexible structures in the dynamic sense. The PMMA chains might not be packed so tightly in the core as the heterocontacts are forbidden between the PS and PMMA elements, which follows that the PMMA core might spread out in the micelle with a respectable size.

Micellar Structure. The apparent mean-square radius of gyration of the mixture, $\langle S^2\rangle^*$, is given by eq A26. Substituting the values obtained experimentally or calculated as $\langle S^2\rangle^* = (R_G^*)^2 = 2.87 \times 10^{-11}$ (cm^2), $\gamma_u M_u/M_{w,mix} = 1/5$, and $\gamma_m M_m/M_{w,mix} = 4/5$ into eqs A18 and A26, we have

$$P(\theta) = 0.20P_u(\theta) + 0.80P_m(\theta) \tag{17}$$

$$[0.20h^2 + 0.80]\langle S^2\rangle_{m,PS} = \langle S^2\rangle^* = 2.87 \times 10^{-11}\ (\mathrm{cm}^2) \tag{18}$$

Here h denotes the size ratio of the unimer to the micelle, and $M_{w,mix}$ is the molecular weight of the mixture. Under the assumption that unimers and micelles are of the same shape and structure, i.e., a hollow corona, it follows that

$$h \equiv [\langle S^2\rangle_{u,PS}/\langle S^2\rangle_{m,PS}]^{1/2} \equiv R_{Gu,PS}/R_{Gm,PS} = R_{Gu}/R_{Gm} = R_{Hu}/R_{Hm} \tag{19}$$

Here R_{Gm} and R_{Hm}, respectively, mean the radius of gyration and the Stokes radius of the hollow corona micelle since the outer corona part alone contributes to the radius of gyration of the hollow shape structured particle, i.e., $\langle S^2\rangle_{m,PS} = \langle S^2\rangle_m = R_{Gm}2$. Equation 18, when combined with the experimental value $R_{Hu}/R_{Hm} = 0.370$, gives that $\langle S^2\rangle_{m,PS} = 3.47 \times 10^{-11}$ cm^2 (or $R_{Gm,PS} = R_{Gm} = 58.9$ nm) and that $R_{Gm}/R_{Hm} = 1.23$. The latter ratio, which is much larger than $(3/5)^{1/2}$ for rigid spheres, indicates that the present micelle is not of hard spheres. This result is consistent with the aspect of the intramicellar motions mentioned already. From this viewpoint, it is worthwhile to analyze the $P(\theta)$ data under an assumption that the micelle is of the hollow structure composed of the spherical soft core and the corona of n rays of Gaussian chains,[29,30] since the simple hollow-sphere models proposed so far failed to explain the present $P(\theta)$ data. Let the core radius be r_c and the mean-square radius of gyration of a Gaussian chain be $\langle S^2\rangle_{SG}$. Here we express the latter by the chain diameter D as $D = 2\langle S^2\rangle_{SG}^{1/2}$. The mean-square radius of gyration of the outer corona $\langle S^2\rangle_o$ is then given by the sum of the intrachain dimension $\langle S^2\rangle_{o1}$ and the interchain dimension $\langle S^2\rangle_{o2}$ as[29,30]

$$\langle S^2\rangle_o = (1/n)\langle S^2\rangle_{o1} + (1 - 1/n)\langle S^2\rangle_{o2} \tag{20}$$

$$\langle S^2\rangle_{o1} = \langle S^2\rangle_{SG} = D^2/4$$

$$\langle S^2\rangle_{o2} = 4\langle S^2\rangle_{SG}\{(3/4) + (r_c/D)^2 + (7/3\pi^{1/2})(r_c/D) \times [1 + (9\pi^{1/2}/14)(r_c/D)]/[1 + (2/\pi^{1/2})(r_c/D)]\} \equiv D^2F(r_c/D) \tag{21}$$

For the present micelle, $\langle S^2\rangle_{m,PS}$ is equal to $\langle S^2\rangle_o$ and can be written by the PS chain diameter D_m and the core radius r_{cm} as

$$\langle S^2\rangle_{m,PS} = R^2_{Gm,PS} = D_m{}^2[1/4n + (1 - 1/n)F(r_{cm}/D_m)] \tag{22}$$

Since the unimer and the micelle have structural similarity, eq 22 holds also for the unimer dimension

$$\langle S^2\rangle_{u,PS} = R^2_{Gu,PS} = D_u{}^2[1/4n + (1 - 1/n)F(r_{cu}/D_u)] \tag{23}$$

where a single PS chain is replaced by n rays of the hypothetical Gaussian chains. The structural similarity of the model gives the relation $r_c/D = r_{cu}/D_u = r_{cm}/D_m$, which turns out to be $D_u/D_m = R_{Gu}/R_{Gm} = h$ from eqs 19, 22, and 23.

The particle scattering factor for the hollow Gaussian corona $P_0(\theta)$ is the sum of the Debye functions for a single Gaussian chain $P_{01}(\theta)$ and the interchain interference $P_{02}(\theta)$[29,30]

$$P_0(\theta) = (1/n)P_{01}(\theta) + (1 - 1/n)P_{02}(\theta) \tag{24}$$

$$P_{01}(\theta) = (2/x^2)[\exp(-x) - 1 + x] \qquad x = q^2\langle S^2\rangle_{SG} = (qD)^2/4$$

$$P_{02}(\theta) = 4(1 + 2r_c/D\pi^{1/2})^{-1}\int_{rc/D}^{\infty}\{r[1 - erf(r - r_c/D)] - (r_c/D)\times[1 - erf(2r - 2r_c/D)]\}[\sin(qDr)/qDr]\mathrm{d}r \tag{25}$$

$P_m(\theta)$ and $P_u(\theta)$ can be obtained from $P_0(\theta)$ by replacing D with D_m and $D_u = hD_m$, respectively. Then, $P(\theta)$ in eq 17 becomes a function of h, n, r_c/D, and D_m, under the conditions of eqs 18 and 22−25. With $\langle S^2\rangle_{m,PS} = 3.47 \times 10^{-11}$ cm^2 (or $R_{Gm,PS} = R_{Gm} = 58.9$ nm) and $h = 0.370$ (= R_{Hu}/R_{Hm} in Table 2), the experimental $P(\theta)$ data were fitted successfully to the model $[P(\theta)]_{calc}$ for the hollow Gaussian chain, where the association number of the micelle z and a set of r_c/D and D_m were changed systematically. Figure 7 shows the results, where the data and the calculated values are given, respectively, in terms of $\{[Kc/R(\theta)]_{c=0}\}^{1/2}$ (unfilled circles) and the broken line estimated by $\{[Kc/R(\theta)]_{c=0,calc}\}^{1/2} = 1/\{M^*[P(\theta)]_{c=0,calc}\}^{1/2}$ with M^* the apparent molecular weight $M^* = 1.23 \times 10^6$. The broken line is the best-fitted result to the data with $z = 3$, $r_c/D = 0.50$, and $D_m = 54.0$ nm. It should be noted here that the association number of the micelle $z = 3$ was optimum, and that the larger z reduced drastically the goodness of the data fitting. Thus, the assumption of $z = 3$, which was made a priori in the previous section, was verified. In the micelle, the size of the Gaussian corona is found to be two times larger than the core radius. The structure parameters obtained above are verified also by the following result: the amplitude ratio of the unimer to the micelle, $f_{II}(\theta)/[f_I(\theta) + f_{III}(\theta)]$ obtained experimentally at $\theta \geq 90°$, was reproduced to within ±10% from the theoretical expression $f_{II}(\theta)/[f_I(\theta) + f_{III}(\theta)] = 0.25[P_u(\theta)/P_m(\theta)]_{calc}$ given

in eqs A21 and A23. All of the characteristics of micelles and unimers are summarized in Table 2.

Intrinsic Viscosity. As summarized in Table 3, the intrinsic viscosity $[\eta]$ of BMM313 in the mixed solvent of $\phi_{bz} = 0.40$ is 210 cm^3g^{-1}. This value is nearly one half of 411 cm^3g^{-1} of a single copolymer BMM313 in BZ and is larger only by 15% than 184 cm^3g^{-1} of the precursor PS in BZ. On the other hand, the single BMM313 (unimer) and micelle coexist in this mixed solvent and their Stokes radii R_H are 17.7 and 47.8 nm, respectively, with the weight fraction of micelles $\gamma_m = 4/7$. The R_H for the micelle is unexpectedly large when compared with $R_H = 35.0$ nm for the single BMM313 in BZ. These facts contradict with viscosity data. We have no way to explain *statically* the decrease of $[\eta]$ in the mixed solvent since we have already considered the effect of preferential adsorption on the molecular characteristics of this system. A possible explanation would be made in a *dynamic* way. As verified by various facts discussed in the previous sections, the present micelle is a loose association composed of small numbers of BMM313. Such an association would fall into pieces under shear flow, because the shear rate $\dot{\gamma}$ was 1700−2000 s^{-1} in the present capillary viscometer. In fact, the shear-broken association in dilute solution has already been detected for cellulose diacetate in polar solvents at shear rate as low as $\dot{\gamma} = 990$ s^{-1}, although the associations were detected *statically*, or by light scattering, in the quiescent state.[31] In addition, the shear-thinning phenomenon has been observed in a dilute solution of block copolymers in poor solvents around the phase separation/precipitation region.[32] These studies would support the possibility proposed above, that is, only the single-block copolymer disperses molecularly in the shear flow of the capillary viscometer.

In conclusion, $[\eta]$ in the mixed solvent of $\phi_{bz} = 0.40$ is the value for a single BMM313 but not for a micelle. We then have a reasonable picture, from the viscosity point of view, for the solutions of this mixed solvent. As shown in the middle lines in Table 2, we can estimate the corresponding viscometric radius R_V, and compare it with other R_V for BMMA and PS in pure BZ. It then follows that the single BMM313, which takes a corona-core structure, shrinks down to the radius of $R_V = 37.1$ nm in the mixed solvent. This R_V value corresponds to an 80% value in pure BZ ($R_V = 46.3$ nm) but is still by 37% larger than that of the precursor homo-PS ($R_V = 24.3$ nm) in the mixed solvent.

Conclusion

In a mixed selective solvent of $\phi_{bz} = 0.40$, the PS−PMMA diblock copolymer forms a monodispersed micelle and coexists with the single copolymer (unimer) in the quiescent state. Micellization takes place under the weak segregation condition and leads the micelle to a thermodynamically equilibrium size of loose association, the association being composed of three pieces of unimers. However, the micelle breaks into pieces of unimers at the shear rate of 1700−2000 s^{-1} in the capillary viscometer. The micelle and the unimer take a structure of soft-core/Gaussian chain shell type, not of a hard-core shell type, in equilibrium. The PS shell part contains the excess amount of PCY because of the preferential adsorption effect, while the core part is not so tightly packed by PMMA because a limited amount of BZ was adsorbed. This structure provides vast internal motions in both the unimer and micelle, though the motions can be experimentally detected only for the micelle of larger size. The internal motions are much stronger than those in usual flexible linear polymers in good solvents, and this situation shifts the nondraining q^3 dependence of the internal decay rates to such an extremely low region as $qR_H = 1$.

Appendix

Here we consider a mixture of one kind of unimer (suffix u) and of micelle (m) of an A−B diblock copolymer in a mixed solvent, good (1) and poor/precipitant (2). Let the weight fraction of unimer be γ_u, the weight fraction of the A part in the copolymer be w_A, and the volume fraction of good solvent be ϕ_1 with the conditions that

$$\gamma_u + \gamma_m = 1,\ w_A + w_B = 1 \quad \text{and} \quad \phi_1 + \phi_2 = 1 \tag{A1}$$

Applying to the present system the generalized light scattering expressions for block copolymers,[25,26] where copolymers are polydisperse with respect to molecular weight and structure, and for a single polymer in the binary solvent,[27,28] where the preferential adsorption of good solvents to the polymer causes a modification of the solvent composition in the vicinity of the polymer, we have the following relations for a dilute solution.

Rayleigh Ratio. Let $(x_{A1})_u$ be the excess number of molecules of solvent 1 adsorbed around the A part per solute molecule, or unimer. Under the assumption that no volume change takes place by the selective adsorption, we have

$$\sum_{i=u,m}\{(x_{A1} + x_{B1})v_1 + (x_{A2} + x_{B2})v_2\}_i = 0 \tag{A2}$$

for a solute molecule, or unimer and micelle. Here v_1 and v_2 are the partial molar volumes of the two solvents 1 and 2, respectively, and $\{...\}_u$ means the excess number of solvent molecules adsorbed per unimer particle. The dipole moment with no preferential adsorption p changes to p' as

$$p' = p + \sum_{i=u,m}\{(x_{A1} + x_{B1})p_1 + (x_{A2} + x_{B2})p_2\}_i \tag{A3}$$

where p_1 and p_2 are the dipole moments relative to molecules of solvents 1 and 2. Then, the reduced Rayleigh ratio R can be written as

$$R = (16\pi^4 n_u/\lambda_0{}^4 N_A)[(p/E)_u + (1/E)\{(x_{A1} + x_{B1})_u p_1 + (x_{A2} + x_{B2})_u p_2\}]^2 + (16\pi^4 n_m/\lambda_0{}^4 N_A)[(p/E)_m + (1/E)\{(x_{A1} + x_{B1})_m p_1 + (x_{A2} + x_{B2})_m p_2\}]^2 \tag{A4}$$

with n_u and n_m the number of unimer and micelle molecules per unit volume, respectively, and E the electric field. Here, $(p/E)_u$ is the polarizability of the unimer particle itself and is given by

$$(p/E)_u = (n_0/2\pi)(M_u/N_A)(dn/dc)_{0,\phi 1} \tag{A5}$$

where n_0 and $(dn/dc)_{0,\phi 1}$ are the refractive index of the mixed solvent and the specific refractive index increment in the mixed solvent of ϕ_1 without taking the preferential adsorption into consideration, i.e., the bulk values. M_u is the molecular weight of unimer. Here n_0 is given by

$$(n_0{}^2 - 1)E = 4\pi(n_1 p_1 + n_2 p_2) \tag{A6}$$

with n_1 and n_2 the number of solvent molecules 1 and 2 per unit volume. The preferential adsorption term in eq A4, $\{(x_{A1} + x_{B1})_u p_1 + (x_{A2} + x_{B2})_u p_2\}$, can be written as

$$\{(x_{A1} + x_{B1})_i p_1 + (x_{A2} + x_{B2})_i p_2\} = (x_{A1} + x_{B1})[p_1 - (v_1/v_2)p_2] \quad (i = u, m) \tag{A7}$$

by using eq A2 under the condition that both the unimer and micelle are the same with respect to the state of preferential adsorption, that is, $\{...\}_m \propto \{...\}_u$. Inserting into eq A7 the condition that no change occurs in the total volume of solvents ($n_1v_1 + n_2v_2 = \text{const}$), or the variation in the solvent composition takes place without any change in the volume ($dn_1v_1 + dn_2v_2 = 0$), and further using the relation that $n_u = c_uN_A/M_u$, we have eq A4 as

$$R = (4\pi^2 n_0^2/\lambda_0^4 N_A)\sum_{i=u,m} c_i M_i[(dn/dc)_{0,\phi 1} + \{(x_{A1} + x_{B1})/M_i\}N_A(dn_0/dn_1)]^2$$

Finally it follows that

$$R = K^*\sum_{i=u,m} c_i M_i[(dn/dc)_{0,\phi 1} + \{(x_{A1} + x_{B1})/M_i\}v_1 (dn_0/d\phi_1)]^2 \quad \text{(A8)}$$

with $\phi_1 = n_1v_1/N_A$ and $K^* = 4\pi^2 n_0^2/\lambda_0^4 N_A$. Here, $\{(x_{A1} + x_{B1})/M_i\}v_1$ in the square brackets can be expressed and defined as

$$\{(x_{A1} + x_{B1})/M_i\}v_1 \equiv \alpha_{A1} + \alpha_{B1} \equiv \alpha_1 \quad (i = u, m) \quad \text{(A9)}$$

Here α_1 is called the preferential adsorption parameter that characterizes the variation of solvent composition in the vicinity of the A part (α_{A1}) and the B part (α_{B1}) of the unimer or micelle and represents the excess number of solvent 1 molecules absorbed per unit molecular weight of unimer or micelle. It should be noted from eq A2 that

$$\alpha_{A1} + \alpha_{B1} = -(\alpha_{A2} + \alpha_{B2}) \quad \text{(unimer and micelle)} \quad \text{(A10)}$$

A negative value of α_{A1}, for example, indicates a preferential adsorption not of solvent 1 to the A part, but of solvent 1 to the B part or of solvent 2 to the A or B part. Whereas $dn_0/d\phi_1$, in the square brackets of eq A8, is the variation of the specific refractive index of mixed solvent with the composition and can be determined experimentally.

If the solution of mixed solvents, in which the copolymer micelle coexists with its unimer, is regarded as a solution of a homopolymer (the apparent molecular weight M^*) of the specific refractive index increment ν and of the mass concentration c, we finally have

$$K^*cM^*\nu^2 = K^*\sum_{i=u,m} c_i M_i[(dn/dc)_{0,\phi 1} + (\alpha_{A1} + \alpha_{B1})(dn_0/d\phi_1)]^2$$
$$= K^*\sum_{i=u,m} c_i M_i (dn/dc)_{0,\phi 1}^2[1 + (\alpha_{A1} + \alpha_{B1})\{(dn_0/d\phi_1)/(dn/dc)_{0,\phi 1}\}]^2 \quad \text{(A11)}$$

with $\alpha_{A1} + \alpha_{B1} = -(\alpha_{A2} + \alpha_{B2})$ and the assumption that the unimer and micelle are in the same preferential adsorption state.

Molecular Weight. Equation A11 can be rewritten as

$$M^*\nu^2 = \gamma_u M_u \nu_u^2 + \gamma_m M_m \nu_m^2 \quad \text{(A12)}$$

Here γ_u is the weight fraction of the unimer $\gamma_u = c_u/(c_u + c_m)$ and c_u is the mass concentration of unimer with the normalization of eq A1. Further, we have

$$\nu_u = \nu_m \equiv (dn/dc)_{0,\phi 1}F(\alpha_{A1},\alpha_{B1})$$
$$F(\alpha_{A1},\alpha_{B1}) \equiv 1 + (\alpha_{A1} + \alpha_{B1})\{(dn_0/d\phi_1)/(dn/dc)_{0,\phi 1}\} \quad \text{(A13)}$$

The apparent molecular weight of the mixture, M^*, is then given by

$$M^* = (\nu_{\phi 1}/\nu)^2 M_{w,mix} \quad \text{(A14)}$$

$$M_{w,mix} = \gamma_u M_u + \gamma_m M_m$$
$$\nu_{\phi 1} \equiv \nu_u = \nu_m = (dn/dc)_{0,\phi 1}F(\alpha) \quad \text{(A15)}$$

where $M_{w,mix}$ is the *true* weight average molecular weight of the mixture. The $(dn/dc)_{0,\phi 1}$ of the copolymer (the weight fraction w_A) in the mixed solvent of ϕ_1 can be calculated as

$$(dn/dc)_{0,\phi 1} = \sum_{j=A,B;k=1,2} w_j \nu_{0,jk}\phi_k$$

where $\nu_{0,A1} = (dn/dc)_{0,A1}$, for example, is the specific refractive index increment of homo-A in a single solvent 1.

Particle Scattering Factor and First Cumulant. Under the condition that there is little interparticle interferences and that two solvents 1 and 2 are isorefractive to the B part of the copolymers, i.e., $\nu_{B1} = \nu_{B2} = 0$, the particle scattering factor of the mixture at finite scattering angle θ, $P(\theta)$, can be obtained as an extension[4,25,26] from eq A12

$$P(\theta) = (1/\nu^2 M^*)[\gamma_u M_u \nu_u^2 P_u(\theta) + \gamma_m M_m \nu_m^2 P_m(\theta)] \quad \text{(A16)}$$

where $P_u(\theta)$ or $P_m(\theta)$ is the particle scattering factor that could be measured if the unimer or the micelle exists solely in the solution. Whereas the first cumulant $\Gamma_e(\theta)$ measured by DLS experiments is obtained under the same conditions as

$$\Gamma_e(\theta) = [-d|\ln g^{(1)}(t)|dt]_{t=0}$$
$$= [\gamma_u M_u \nu_u^2 P_u(\theta)\Gamma_u(\theta) + \gamma_m M_m \nu_m^2 P_m(\theta)\Gamma_m(\theta)] \times [\gamma_u M_u \nu_u^2 P_u(\theta) + \gamma_m M_m \nu_m^2 P_m(\theta)]^{-1}$$
$$= [1/\nu^2 M^* P(\theta)][\gamma_u M_u \nu_u^2 P_u(\theta)\Gamma_u(\theta) + \gamma_m M_m \nu_m^2 P_m(\theta)\Gamma_m(\theta)] \quad \text{(A17)}$$

where $\Gamma_u(\theta)$ and $\Gamma_m(\theta)$ are the mean decay rates of the unimer and micelle, respectively. With the equality in the preferential adsorption state for unimer and micelle, that is, $\nu_u = \nu_m \equiv \nu_{\phi 1}$, we have

$$P(\theta) = (\nu_{\phi 1}/\nu)^2[\gamma_u M_u P_u(\theta) + \gamma_m M_m P_m(\theta)]/M^*$$
$$= [\gamma_u M_u P_u(\theta) + \gamma_m M_m P_m(\theta)]/M_{w,mix} \quad \text{(A18)}$$

$$\Gamma_e(\theta) = [(\nu_{\phi 1}/\nu)^2/M^*P(\theta)][\gamma_u M_u P_u(\theta)\Gamma_u(\theta) + \gamma_m M_m P_m(\theta)\Gamma_m(\theta)]$$
$$= [1/M_{w,mix}P(\theta)][\gamma_u M_u P_u(\theta)\Gamma_u(\theta) + \gamma_m M_m P_m(\theta)\Gamma_m(\theta)]$$
$$\equiv f_{II}(\theta)\Gamma_u(\theta) + \{f_I(\theta) + f_{III}(\theta)\}\Gamma_m(\theta) \quad \text{(A19)}$$

Here f_{II} and $f_I + f_{III}$ are the fractional amplitudes of unimer and micelle, respectively, as is described in the histogram analysis of $A(t)$, and are given by

$$f_{II}(\theta) = (\gamma_u M_u/M_{w,mix})[P_u(\theta)/P(\theta)]$$
$$f_I(\theta) + f_{III}(\theta) = (\gamma_m M_m/M_{w,mix})[P_m(\theta)/P(\theta)] \quad \text{(A20)}$$

The ratio is given by

$$f_{II}(\theta)/[f_I(\theta) + f_{III}(\theta)] = \gamma_u M_u P_u(\theta)/\gamma_m M_m P(\theta) \quad \text{(A21)}$$

It should be clearly noticed that the amplitudes are expressed, from eq A18, as

$$P(\theta) = [f_{II}(\theta) + \{f_I(\theta) + f_{III}(\theta)\}]P(\theta) \quad \text{(A22)}$$

and that $\Gamma_u(\theta)$ and $\Gamma_m(\theta)$ in eq A19 are the *true* decay rate values. At $\theta \rightarrow 0$, the intramicellar amplitude should be zero, i.e., $f_{III}(0) = 0$ and $P(0) = P_u(0) = P_m(0) = 1$. Thus, we have $[\Gamma_u(\theta)/q^2]_{q=0} = D_u(0) \equiv D_{II}$ and $[\Gamma_m(\theta)/q^2]_{q=0} = D_m(0) \equiv D_I$, and eqs A19−A21 turn out to be

$$\Gamma_e = f_u(0)D_{II} + f_m(0)D_I$$
$$f_u(0) = \gamma_u M_u/M_{w,mix} = \gamma_u M_u/(\gamma_u M_u + \gamma_m M_m)$$
$$f_m(0) = \gamma_m M_m/M_{w,mix} = \gamma_m M_m/(\gamma_u M_u + \gamma_m M_m)$$
$$f_u(0)/f_m(0) = \gamma_u M_u/\gamma_m M_m \quad \text{(A23)}$$

where the scattering vector $\boldsymbol{q}$ is given by $q = (4\pi n_0/\lambda_0)\sin(\theta/2)$. Equation A23 gives the amplitude ratio of the unimer diffusion to the micellar diffusion.

Radius of Gyration. Under the same conditions as mentioned above, i.e., with little interparticle interference and the isorefractivity of both solvents to the B part of the copolymers, the apparent mean-square radius of gyration of the mixture, $\langle S^2\rangle^*$, is obtained from the general expression of $\langle S^2\rangle^* = -3[dP(\theta)/dq^2]_{q=0}$ as

$$M^*\langle S^2\rangle^* = (1/\nu)^2[\gamma_u M_u \nu_u^2 \langle S^2\rangle_{u,A} + \gamma_m M_m \nu_m^2 \langle S^2\rangle_{m,A}] \quad \text{(A24)}$$

With $\nu_{\phi 1} = \nu_u = \nu_m$, it follows that

$$M^*\langle S^2\rangle^* = (\nu_{\phi 1}/\nu)^2[\gamma_u M_u \langle S^2\rangle_{u,A} + \gamma_m M_m \langle S^2\rangle_{m,A}] \quad \text{(A25)}$$

or

$$M_{w,mix}\langle S^2\rangle^* = \gamma_u M_u \langle S^2\rangle_{u,A} + \gamma_m M_m \langle S^2\rangle_{m,A} = [\gamma_u M_u h^2 + \gamma_m M_m]\langle S^2\rangle_{m,A} \quad \text{(A26)}$$

Here $\langle S^2\rangle_{u,A}$ and $\langle S^2\rangle_{m,A}$ are the real (*true*) mean-square radius of gyration of the A part about its center of gravity for the unimer and micelle, respectively. Then, h^2 represents the size ratio of the unimer and micelle, which can be measured only through the A part, $h^2 = \langle S^2\rangle_{u,A}/\langle S^2\rangle_{m,A}$.

References and Notes

(1) Akcasu, A. Z. *Dynamic Light Scattering. The Method and Some Applications*; Brown, W., Ed.; Clarendon: Oxford, U.K., 1993; Chapter 1.
(2) Akcasu, A. Z.; Nagele, G.; Klein, R. *Macromolecules* **1991**, *24*, 4408.
(3) Benmouna, M.; Benoit, H.; Borsali, R.; Duval, M. *Macromolecules* **1987**, *20*, 2620.
(4) Burchard, W. *Adv. Polym. Sci.* **1983**, *48*, 1.
(5) Burchard, W.; Kajiwara, K.; Nerger, D.; Stockmayer, W. H. *Macromolecules* **1984**, *17*, 222.
(6) Semenov, A. N.; Fytas, G.; Anastasiadis, S. H. *Polym. Prepr. (Am. Chem. Soc.)* **1994**, *35* (1), 618.
(7) Pan, C.; Maurer, W.; Liu, Z.; Lodge, T. P.; Stepanek, P.; von Meerwall, E. D.; Watanabe, H. *Macromolecules* **1995**, *28*, 1643.
(8) Balsara, N. P.; Stepanek, P.; Lodge, T. P.; Tirrell, M. *Macromolecules* **1991**, *24*, 6227.
(9) Tsunashima, Y.; Kawamata, Y. *Macromolecules* **1993**, *26*, 4899.
(10) Tsunashima, Y.; Kawamata, Y. *Macromolecules* **1994**, *27*, 1799.
(11) (a) Tsunashima, Y.; Hirata, M.; Kawamata, Y. *Macromolecules* **1990**, *23*, 1089. (b) Tsunashima, Y. *Macromolecules* **1990**, *23*, 2963.
(12) Honda, C.; Sasaki, K.; Nose, T. *Polymer* **1994**, *35*, 5309.
(13) Honda, C.; Hasegawa, Y.; Hirunuma, R.; Nose, T. *Macromolecules* **1994**, *27*, 7660.
(14) Quintana, J. R.; Janez, M. D.; Villacampa, M.; Katime, I. *Macromolecules* **1995**, *28*, 4139.
(15) Villacampa, M.; Apodaca, E. D.; Quintana, J. R.; Katime, I. *Macromolecules* **1995**, *28*, 4144.
(16) Quintana, J. R.; Villacampa, M.; Katime, I. *Macromolecules* **1993**, *26*, 606.
(17) Siqueira, D. F.; Nunes, S. P.; Wolf, B. A. *Macromolecules* **1994**, *27*, 234, 4561.
(18) (a) Zhou, Z.; Chu, B.; Peiffer, D. G. *J. Polym. Sci. Part B: Polym. Phys.* **1994**, *32*, 2135. (b) Zhou, Z.; Chu, B.; Peiffer, D. G. *Macromolecules* **1993**, *26*, 1876.
(19) Tsunashima, Y.; Suzuki, S., in preparation.
(20) *Organic Solvents*, 3rd ed.; Riddick, J. A., Bunger, W. B., Eds.; Wiley-Interscience: New York, 1970.
(21) Kurata, M. *Bull. Chem. Soc. Jpn.* **1952**, *25*, 32.
(22) Tsunashima, Y.; Nemoto, N.; Kurata, M. *Macromolecules* **1983**, *16*, 584.
(23) Tsunashima, Y.; Hirata, M.; Nemoto, N.; Kurata, M. *Macromolecules* **1987**, *20*, 1992.
(24) Nemoto, N.; Makita, Y.; Tsunashima, Y.; Kurata, M. *Macromolecules* **1984**, *17*, 425.
(25) Benoit, H.; Froelich, D. *Light Scattering from Polymer Solutions*; Huglin, M. B., Ed.; Academic: London, 1972; Chapter 11 (Application of LS to Copolymers).
(26) Kratochvil, P. *Light Scattering from Polymer Solutions*; Huglin, M. B., Ed.; Academic: London, 1972; Chapter 7 (Particle Scattering Functions).
(27) Strazielle, C. *Light Scattering from Polymer Solutions*; Huglin, M. B., Ed.; Academic: London, 1972; Chapter 15 (LS in Mixed Solvents).
(28) Ewart, R. H.; Roe, C. P.; Debye, P.; McCartney, J. R. *J. Chem. Phys.* **1946**, *14*, 687.
(29) Hirata, M.; Tsunashima, Y. *Macromolecules* **1989**, *22*, 249.
(30) Tsunashima, Y.; Hirata, M.; Kurata, M. *Bull. Inst. Chem. Res., Kyoto University* **1988**, *66*, 184.
(31) (a) Kawanishi, H.; Tsunashima, Y.; Horii, F. *J. Chem. Phys.* **1998**, *109*, 11027. (b) Tsunashima, Y.; Kawanishi, H. *J. Chem. Phys.* **1999**, *111*, 3294.
(32) Tsunashima, Y., to be published.